

Article

Predicting Spruce Taiga Distribution in Northeast Asia Using Species Distribution Models: Glacial Refugia, Mid-Holocene Expansion and Future Predictions for Global Warming

Kirill Korznikov ^{1,2} , Tatyana Petrenko ², Dmitry Kislov ², Pavel Krestov ²  and Jiří Doležal ^{1,3,*} ¹ Department of Functional Ecology, Institute of Botany CAS, 379 01 Třeboň, Czech Republic² Department of Geobotany, Botanical Garden-Institute FEB RAS, 690024 Vladivostok, Russia³ Department of Botany, Faculty of Science, University of South Bohemia, 370 05 České Budějovice, Czech Republic

* Correspondence: jiriddolezal@gmail.com

Abstract: Spruce taiga forests in Northeast Asia are of great economic and conservation importance. Continued climate warming may cause profound changes in their distribution. We use prognostic and retrospective species distribution models based on the Random Forest machine learning method to estimate the potential range change of the dominant taiga conifer Jezo spruce (*Picea jezoensis* (Siebold & Zucc.) Carrière) for the year 2070 climate warming scenarios and for past climate epochs—the Last Glacial Maximum (LGM) (~21,000 years before present) and the mid-Holocene Climatic Optimum (MHO) (~7000 years before the present) using the MIROC-ESM and CCSM4 climate models. The current suitable climatic conditions for *P. jezoensis* are estimated to be 500,000 km². Both climatic models show similar trends in past and future ranges but provide different quantitative areal estimates. During the LGM, the main part of the species range was located much further south than today at 35–45° N. Projected climate warming will cause a greater change in the distributional range of *P. jezoensis* than has occurred since the MHO. Overlapping climatic ranges at different times show that the Changbai Mountains, the central parts of the Japanese Alps, Hokkaido, and the Sikhote-Alin Mountains will remain suitable refugia for Jezo spruce until 2070. The establishment of artificial forest stands of *P. jezoensis* and intraspecific taxa in the future climate-acceptable regions may be important for the preservation of genetic diversity.

Keywords: climate change; boreal forest; spruce forest; *Picea jezoensis*; species distribution modeling; Last Glacial Maximum; Northeast Asia



Citation: Korznikov, K.; Petrenko, T.; Kislov, D.; Krestov, P.; Doležal, J. Predicting Spruce Taiga Distribution in Northeast Asia Using Species Distribution Models: Glacial Refugia, Mid-Holocene Expansion and Future Predictions for Global Warming. *Forests* **2023**, *14*, 219. <https://doi.org/10.3390/f14020219>

Academic Editors: Daniela Dalmonech, Alessio Collalti and Gina Marano

Received: 20 December 2022

Revised: 17 January 2023

Accepted: 20 January 2023

Published: 24 January 2023



Copyright: © 2023 by the authors. Licensee MDPI, Basel, Switzerland. This article is an open access article distributed under the terms and conditions of the Creative Commons Attribution (CC BY) license (<https://creativecommons.org/licenses/by/4.0/>).

1. Introduction

Current climate changes in the boreal zone of Eurasia have led to visible changes in vegetation cover due to increased fire frequency, the proliferation of insect pests, desiccation, and wind disturbances, which alter the structure of the vegetation cover and the distribution of plants and whole biomes [1]. However, it remains unclear how current changes in the distribution of boreal forests and their dominant species deviate from long-term dynamics and what the prospects are. Studying the spatial distribution of dominant species in changing boreal forests can therefore help us better understand the factors behind their past and present occurrence, assess possible climate-induced range shifts, and predict future forest dynamics [2,3].

Recently, species distribution modeling (SDM) methods have been widely used to study the effects of climate change on species ranges [4–7]. Using data on the current distribution of climatic indicators characterizing species range, it is possible to predict climatically suitable areas under current climatic conditions, under climatic conditions of the past, or predicted climatic conditions of the future [8–11]. Identifying areas and climates that have been able to sustain relict populations of dominant boreal species from

the Last Glacial Maximum (LGM) to the present and will be able to sustain them in the future are important for the establishment of protected reserves, as these areas have the potential to contain populations with a continuous history of several tens of thousands of years. This is important for maintaining genetic diversity [12] and further opens the possibility of adaptive management in areas such as forestry and agriculture as well as ex situ species conservation [13,14].

One of the most important taiga forest species for the ecosystem's functioning and timber industry in Northeast Asia is *Picea jezoensis* (Siebold & Zucc.) Carrière (Jezo or Yezo spruce, by the old name of Hokkaido Island), also known as *Picea ajanensis* Fisch. ex Carrière (Ajan spruce) [15]. *P. jezoensis* is a coniferous evergreen tree up to 35 m tall and 120 cm in diameter at breast height. The life expectancy of the trees is 300–400 years; the maximum age is 520 years [16]. Phylogenetically and ecologically, *P. jezoensis* is close to the North American *P. sitchensis* (Bong.) Carrière. This conclusion is also supported by the fact that both *P. jezoensis* and *P. sitchensis* have flattened leaves and loosely arranged seed scales [17]. *P. jezoensis* occurs in the sub-maritime and maritime areas of Northeastern Asia between 40° N and 55° N, where it forms zonal forests [18].

P. jezoensis forms mono-dominant or mixed spruce–fir stands (with *Abies nephrolepis* (Trautv.) Maxim. in the mainland area and *A. sachalinensis* (F.Schmidt) Mast. in the insular part of the region) from the elevation of sea level to 1500–2000 m, depending on latitude. Forests formed by *P. jezoensis* occupy almost the whole range of ecologically different sites in this belt, except only in mires and on rock outcrops. The optimal climatic parameters for this species include a mean annual temperature from -1 to 0 °C, a vegetative period of 145–155 days, and a mean summer precipitation of 370–590 mm. Mean annual air humidity within the range of species does not fall below 60%. The climatic optimum of *P. jezoensis* is thus much more severe than that of European species *Picea abies* (L.) H.Karst. [15,16].

In the most productive spruce forests, timber stock reaches 1000 m^3 with over 500 Mg ha^{-1} of aboveground biomass [15,16]. Due to its high economic potential, *P. jezoensis* is one of the region's main objects of logging and timber production. Besides logging, spruce forests are also affected by natural disturbances. Since the middle of the 20th century, particularly active processes of natural desiccation of *P. jezoensis* primeval forests have been recorded in the continental part of the Far East, with a total area of $55,000\text{ km}^2$ already in the 1970s [16].

The critically important ecosystem function of *P. jezoensis* and the high economic value of this species in the context of current trends in boreal forest degradation due to climate change [19–21] make understanding the *P. jezoensis* range changes by projected climate change scenarios particularly important. Retrospective modeling over time of significant milestones of evolutionary vegetation dynamics, i.e., the LGM (~21,000 years before the present) and the mid-Holocene Climatic Optimum (MHO) (~7000 years before the present), is interesting for assessing the movement of *P. jezoensis* climate optimum in Northeast Asia. There is a clear relevance to paleoenvironmental and phylogenetic studies as well as the understanding of current trends in biodiversity and biome distributions [22].

In this study, we build the SDMs of *P. jezoensis* using the distribution data of the species in its natural habitats (not under culture or plantation conditions) and the WorldClim 1.4 climate dataset [23] associated with the downscaled paleoclimate data [24]. Using paleoclimate data MIROC-ESM [25,26] and CCSM4 [27], we reconstruct the spatial distribution of areas with climatic conditions suitable for *P. jezoensis* in the LGM and MHO. We also construct prognostic models of the potential distribution for 2070 under the RCP2.6 (representative concentration pathway) climate change scenarios [28] and RCP8.5 [29]. We used the MIROC-ESM and CCSM4 models because they cover paleoclimates and predicted future climates among other climatic models. Both prognostic and retrospective SDMs were developed using ensembles of decision trees. Tree-based supervised learning algorithms are quite efficient tools for handling complicated decision boundaries in multifactor spaces [30]. Another advantage of decision trees and their ensembles for SDMs is the ability to estimate the importance of climatic variables and the impacts on the observed species distribution. We focused on building SDMs using the RF classifier (a versatile machine

learning algorithm) and the investigation of overlapping ranges of potential species occurrence under the LGM and projected future climates (RCP2.6, RCP8.5) which could be considered long-term *P. jezoensis* refugia.

2. Materials and Methods

2.1. Study Area

The dark coniferous forests of *P. jezoensis* are widespread from the mountainous regions of central Japan and South Korea in the south to central Kamchatka in the north. The species range extends in latitude from 40° N to more than 55° N [18]. Details of the species biology and ecology are described in previous works [15,16,18,31]. Clarification of intraspecific taxonomy was performed based on allozyme analysis [32,33] and nuclear and organelle DNA [34,35]. We suppose that the single subspecies of *P. jezoensis* subsp. *jezoensis* exists throughout the entire range, except for isolated relict populations in the mountains of central Honshu, attributed to the taxon *P. jezoensis* subsp. *hondoensis* (Mayr) P.A. Schmidt.

The range of *P. jezoensis* includes part of the Primorye Region, the southeast coast of the Sea of Okhotsk, Sakhalin Island, the southern islands of the Kuril Archipelago, part of Northeast China, central Kamchatka (the so-called “coniferous forest island”), the north of the Korean Peninsula, Hokkaido Island, and the central part of Honshu Island (Figure 1) [15,18]. The range of *P. jezoensis* lies in a deeply rugged mountain area. The climate in the area of the *P. jezoensis* range is controlled by the seasonally alternating maritime and continental air masses brought about by monsoon circulation. Annual precipitation ranges from 460 mm in central Kamchatka to 1250 mm in the southern Kuril Islands, and average annual temperatures range from −3 °C in the continental part to +7.5 °C in Hokkaido. The influence of the East Asian monsoon decreases with distance inland. In the continental part of the range, winters are sparsely snowy and cold, while summers are cool and humid. Mean annual air humidity within the range of *P. jezoensis* does not fall below 60%, although it varies considerably from region to region. Summarizing climatic conditions in the areas where *P. jezoensis* forms pure and fir-mixed stands, the climatic optimum is much harsher than for European *P. abies*. [15].

The presence of refugia both in the northern part of the range (isolated populations in Kamchatka) and in the southern part (isolated populations in the mountains of South Korea and *P. jezoensis* ssp. *hondoensis* in the Japanese Alps) testifies to an extensive shifting of the species range in the past associated with periods of warming and cooling in the Pleistocene. Thus, the explanation of the modern range of *P. jezoensis* lies not only in the current climatic conditions of the present but also in its changes over the past millennia. This is confirmed, among other things, by modern population genetics data [34,35].

2.2. Presence Points

Georeferenced occurrence points of *P. jezoensis* were taken from different sources: 1—local herbarium collections of the Botanical Garden-Institute FEB RAS (herbarium acronym VBGI) and Institute of Biology and Soil Science FEB RAS (VLA); 2—Global Biodiversity Information Facility database (GBIF) [36]; 3—own archival data of geobotanical relevés and occurrences points sampled in the field research. To create the models, we used only those points of *P. jezoensis* presence that belong to *P. jezoensis* subsp. *jezoensis*, i.e., not including *P. jezoensis* subsp. *hondoensis*, whose relict populations are isolated from the contiguous range of this species in the mountains of central Honshu.

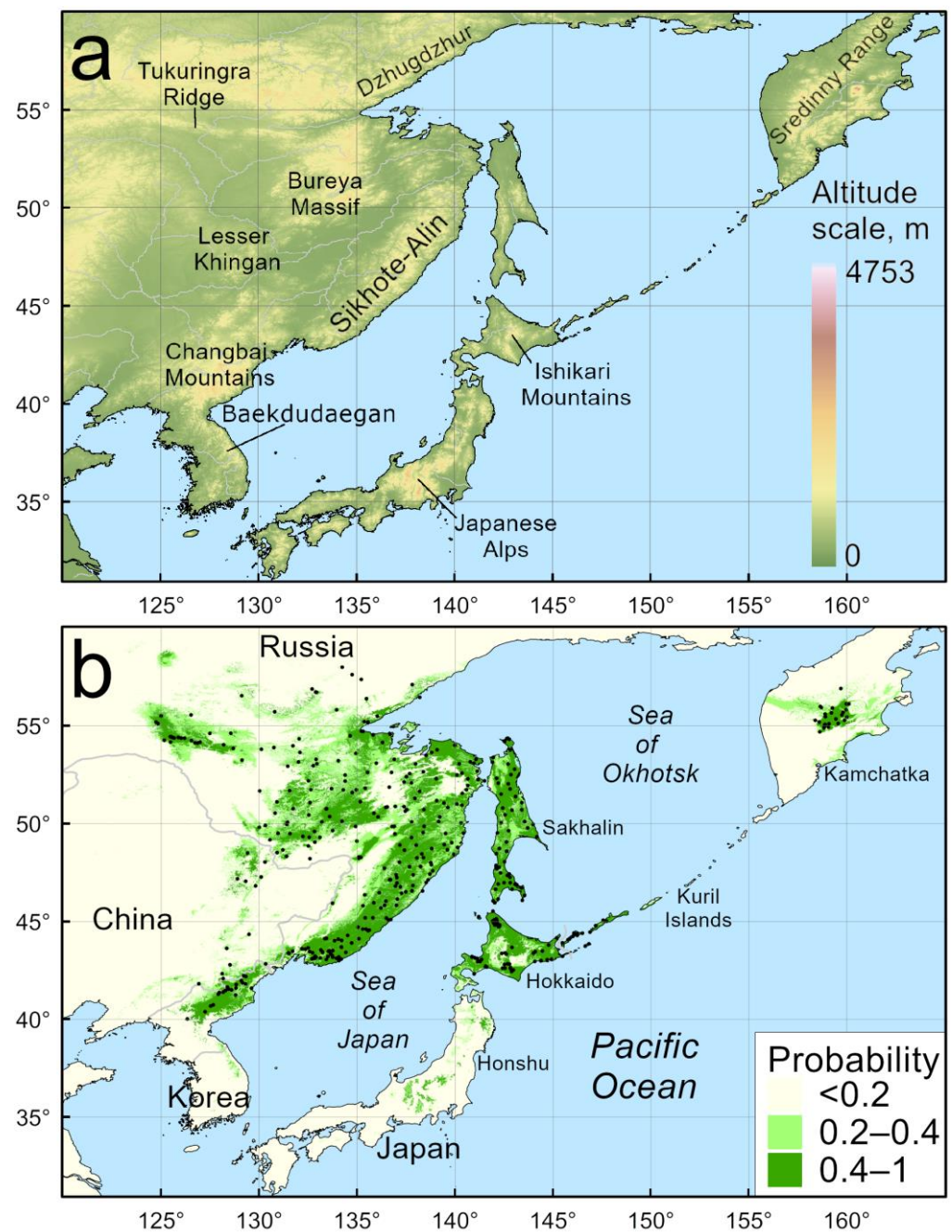


Figure 1. Topography map of the region (a), the built species distribution model of *Picea jezoensis* (Siebold & Zucc.) Carrière represented as a probability map; black dots indicate presence points in the model train ($n = 479$) (b).

The presence of points outside the natural distribution area (forest plantations on the islands of Hokkaido and Sakhalin) and in urbanized areas (gardens, parks) was excluded using high-resolution satellite images. A filtering algorithm was then applied to remove presence points located closer to each other than 2 km apart. The algorithm was implemented using the geopy package [37]. We then calculated the average nearest neighbor index implemented in the ArcMap 10.8 program [38] for the remaining data which compares the observed average distance between all presence points to the expected distance for a set of evenly distributed points. If the index is less than 1, the pattern exhibits clustering; if the index is greater than 1, the trend is toward dispersion or competition. Thus, we managed to avoid significant data imbalance effects when one region could be represented

by a disproportionately large number of presence points. As a result, 479 unique points of species presence were used in the modeling (Figure 1b). The number of pseudo absence points randomly placed throughout the simulation area was estimated to be 2 times greater than the number of presence points.

2.3. Climatic Data

To model the distribution of *P. jezoensis*, we used the 5 most informative bioclimatic indices from a set of more than 30 indices provided by [39,40]: Kira's warmth index (WKI, the sum of average monthly temperatures above +5 °C), which showed the highest contributions to the distribution of *P. jezoensis* vegetation in Northeast Asia; Kira's coldness index (CKI, the sum modulo of average monthly temperatures below +5 °C); the index of continentality (IC, difference between annual maximum and minimum average monthly temperatures); the rain precipitation index (Pp, the amount of precipitation during the period with positive average monthly temperatures); and the snow precipitation index (Pn, the amount of precipitation in the period with negative average monthly temperatures) [40]. We conclude that it is better to choose a few predictors with a clear biological interpretation than to select a slightly optimal subset of predictors that have an implicit or unclear impact on species distribution [11].

Preconditions checked before training the classifier included a multicollinearity check of selected bioclimatic indices using NumPy package for Python [41] and the "omcdiag" function from the mctest R-package [42]. The combination of selected bioclimatic indices led to significantly different than zero values of the determinant of the covariance matrix ($p < 0.05$). The index values were calculated from monthly mean temperatures and total precipitation data provided in the WorldClim v.1.4 [23] with a spatial resolution of 30 arc-seconds ($\sim 0.0083^\circ$), which were extracted from the source data files using the Geospatial Data Abstraction Library [43]. Similar data presented in the MIROC-ESM [25,26] and CCSM4 [27] climate models were used to reconstruct the climatic situation during the LGM and MHO and to forecast the climatic situation for the year 2070. Prognostic modeling was performed in accordance with two global climate change scenarios: 1—RCP2.6 implies an increase in the average planetary temperature of 0.3–1.7 °C by 2100 [28]; 2—RCP5 implies an increase of 2.6–4.8 °C [29].

2.4. Model Building

The formal side of SDM consists in finding nonlinear relationships between species distribution and bioclimatic parameters. To handle this problem, we chose the Random Forest (RF) machine learning method implemented in the Python programming language in the Scikit-learn package [44]. We selected RF as a method to build the models following the results of several studies indicating that RF may be more applicable in predicting the native potential distribution of species with sufficient species occurrence data [45,46]. Scikit-learn is a general-purpose machine learning package focused on rapid prototyping, validating, and deploying supervised and unsupervised learning models. It is widely used in the data science world and allows researchers to formulate the process of building SDMs at a high level of abstraction. Using Scikit-learn, the SDM creation process is expressed as a piece of code in Python programming language, which efficiently performs all the necessary steps related to machine learning model development, such as feature engineering and feature selection, training, and model testing phases. We used a grid search cross-validation procedure to find the optimal subset of RF hyperparameters. As a result, optimal values for the configuration parameters of the RF algorithm were found to be equal to the values used in similar models [47]. The optimal number of random trees was found to be equal to 100 and the maximum tree depth was limited to 10. The remaining RF parameters were set to their default values.

The constructed model was evaluated using the continuous Boyce index [48], which is calculated using only species presence points, based on 100 iterations by randomly dividing the original spatial data set into training (3/4 points) and test (1/4 points) data

sets. Using the continuous Boyce index to assess model quality is preferable to using ROC AUC because it is based solely on empirical data on the location of species sites, without reference to pseudo presence points [49].

We evaluated the contribution of each of the five predictors to the final model using the “feature_importances” attribute [50] implemented for the RF from Scikit-learn [44].

The result of applying the trained classifier to climatic data is a probability map (from 0—presence is unlikely to 1—the maximum probability of presence) of habitat suitability for *P. jezoensis*. For practical purposes, such as calculating the area of territory that a species can potentially occupy, we represented the probability maps in binary form, namely “species absent” (0) or “species present” (1). Binary probability maps require finding the optimal threshold value. If the probability in each point exceeds the threshold value, we convert it to 1 and treat it as a “species presence” point. Otherwise, the probability value is converted to 0 and the corresponding point is considered a “species absence” point.

To estimate the optimal threshold value, we considered the problem of maximizing the mean value of maxSSS [51], calculated based on 100 random splits of the original spatial data set into training (3/4) and test (1/4) data sets. A similar optimization issue was noted when compared to actual skill statistics and the F1 score metric (a measure of accuracy, the harmonic mean of precision and recall). To verify the obtained optimal threshold value, we used an expert approach [51,52]. Based on computational experiments, we concluded that the optimal maxSSS yield values for the *P. jezoensis* distribution maps are consistent with the expert evaluation. Binarization using an optimal threshold calculation is a convenient way of quantification, but this approach is not the only one possible; the overall interpretation of the ranges is also important [11]. To this end, we created potential distribution maps with probability levels of 0.4–1 and 0.2–0.4.

Thus, the process of creating the SDM using the RF classifier consisted of the following phases: (1) collection of *P. jezoensis* occurrence data; (2) data preprocessing (removal of duplicates, local equalization of point density, generation of pseudo-absence points); (3) applying recursive feature elimination and expert-based feature selection; (4) grid search for the best set of model parameters (number of trees, tree depth, available trees building criterion); (5) finding the best threshold value (by maximizing maxSSS and expert-based approach); and (6) applying the model to past, present, and future climatic data to result in interpretation.

Finally, we calculated response curves for each model predictor. Response curves are essentially smooth estimates of the modeled probability of species occurrence for a fixed value of a particular predictor. Higher values on the response curves correspond to a higher probability of species occurrence and suitability of climate.

All distribution maps were built in ArcMap 10.8. The relief map was drawn using elevation data from the Shuttle Radar Topography Mission (SRTM) [53].

3. Results

Verification of decision trees by cross-validation of the obtained models of the modern distribution of *P. jezoensis* showed high predictive accuracy. The continuous Boyce index value for all models was 0.99, indicating their high prognostic abilities; the AUC value was 0.89 ± 0.004 ; the maxSSS was 1.696 ± 0.179 ; and the accuracy was 0.932 ± 0.019 . Using the five selected bioclimatic factors as predictors, the most important predictors are related to moisture rather than temperature. The absence of strong differences in the contribution of the factors generally indicates their common high importance in constructing the model (Table 1).

The binarization probability level according to the maxSSS optimal threshold value is 0.43. The climatic ranges of *P. jezoensis* distribution correspond well to the species distribution from ground-based data. A comparison of the distribution model of *P. jezoensis* (Figure 1) with expert range maps of the species shows a high degree of agreement, thus allowing the model of the current climatic range of the species to be used for retrospective and predictive modeling. The inferred climatic ranges of *P. jezoensis* distribution corresponded well to the distribution maps of the species derived from ground-based expert

surveys (Figure S1) [16,18,35]. Cartographic models of the area potentially suitable for *P. jezoensis* for different climatic conditions are shown in Figure 2.

Table 1. Importance of the climatic predictors in the Random Forest model.

Model Predictor	Importance (Mean \pm SE, $n = 100$)
Pp	0.234 \pm 0.010
Pn	0.234 \pm 0.009
WKI	0.210 \pm 0.005
CKI	0.164 \pm 0.003
IC	0.158 \pm 0.001

Pp—annual precipitation in the months with the positive mean temperature; Pn—annual precipitation in the months with the negative mean temperature; WKI—Kira’s warmth index; CKI—Kira’s coldness index; IC—index of continentality.

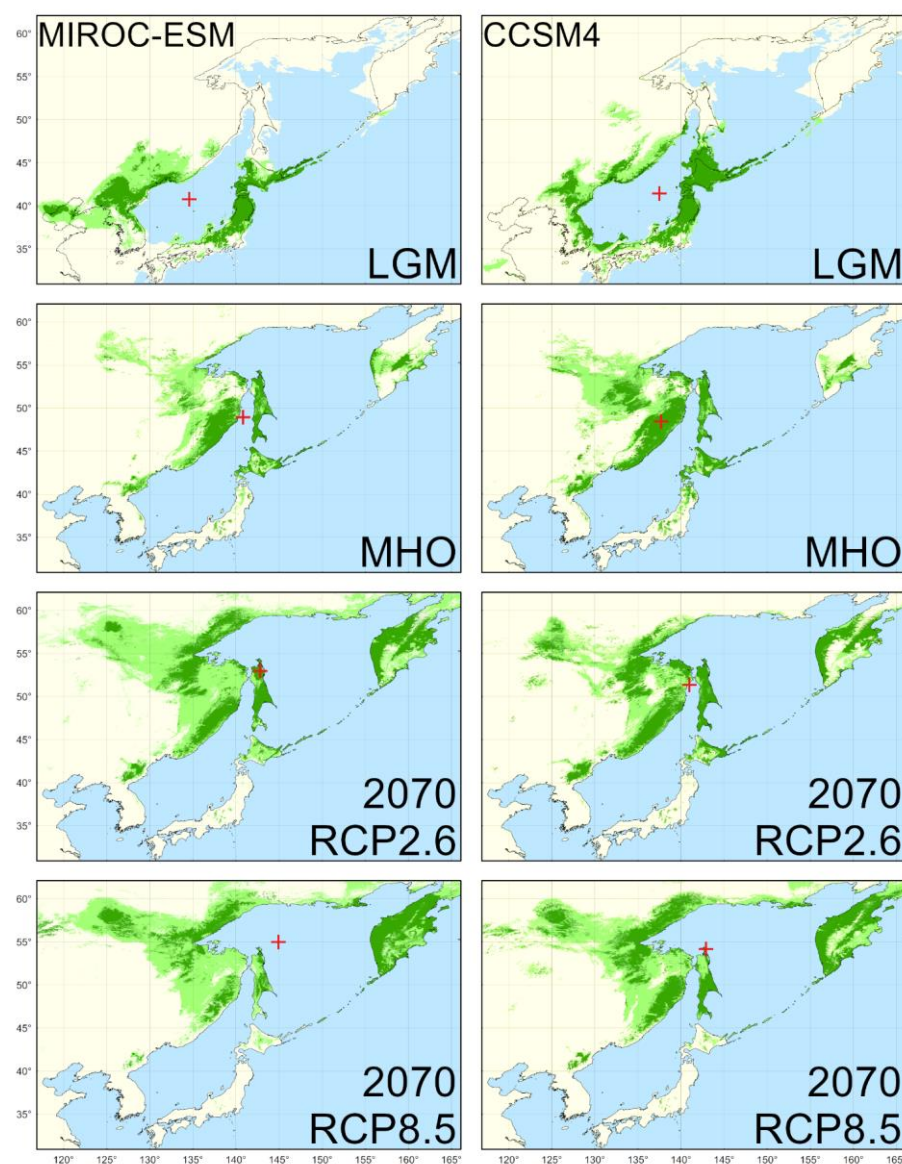


Figure 2. Potential distribution of *Picea jezoensis* (Siebold & Zucc.) Carrière built using the MIROC-ESM and CCSM4 climatic models under the Last Glacial Maximum (LGM), the mid-Holocene Climatic Optimum (MHO), and 2070 RCP2.6 and RCP8.5 scenarios; red crosses indicate the central geographical points of the predictable distributions.

The potential distribution area of *P. jezoensis* is estimated at 513,000 km² in current climate conditions. Quantification of the climatically suitable area of *P. jezoensis* in the LGM, the MHO, and climate projections for the year 2070 are shown in Table 2. Both the MIROC-ESM and CCSM4 climate models showed similar trends in past and future climatic range patterns but provide different quantitative areal estimates. Based on the MIROC-ESM climate model, the potential area of suitable climate conditions of *P. jezoensis* was predicted to be the highest in the 2070-year RCP2.6 scenario and lowest in the MHO (Table 3). Based on the CCSM4 climate model, the potential area of suitable climate conditions of *P. jezoensis* was predicted to be the highest in the 2070-year RCP8.5 scenario and lowest in the MHO. In addition to reflecting similar trends in bioclimatic ranges, the two models are different from each other in terms of quantitative areal estimates: the MIROC-ESM predicted area is significantly (~100,000 km²) smaller than that of CCSM4 (Figure 2).

Table 2. The potential area (km²) of highly suitable climate conditions of *Picea jezoensis* (Siebold & Zucc.) Carrière.

Scenario	CCSM4	MIROC-ESM
LGM	546,250 *	456,471
MHO	494,278	322,155
RCP2.6	614,347 *	581,760 *
RCP8.5	625,076 *	483,805

* Asterisks indicate an increase in the potential area in comparison to the current distribution.

Table 3. The estimation of the overlapped area with the LGM time to the 2070-year climate condition.

Climate Model	Scenario	MIROC-ESM
MIROC-ESM	RCP2.6	18,293
	RCP8.5	4480
CCSM4	RCP2.6	54,725
	RCP8.5	20,416

During the LGM, the main part of the species range was located much further south than today at 35–45° N. Projections for the MHO indicate a retreat from southern territories and northward expansion with a distribution center shifted to 45–55° N.

The SDMs of *P. jezoensis* from the LGM to the year 2070 superimposed on each other revealed the geographical locations where *P. jezoensis* always had favorable conditions. The intersection of potential areas occupied by this species in different periods showed the location of long-term stable refugia. Overlapping climatic ranges at different times showed that the Changbai Mountains, the central parts of the Japanese Alps, the Hokkaido mountains, and the Sikhote-Alin Mountains were the areas where *P. jezoensis* persisted over time. These mountain areas indicate the existence of long-term stable refugia (Figure 3) that deserve the highest priority in the conservation of the *P. jezoensis* gene pool and are expected to be represented by the most ancient populations.

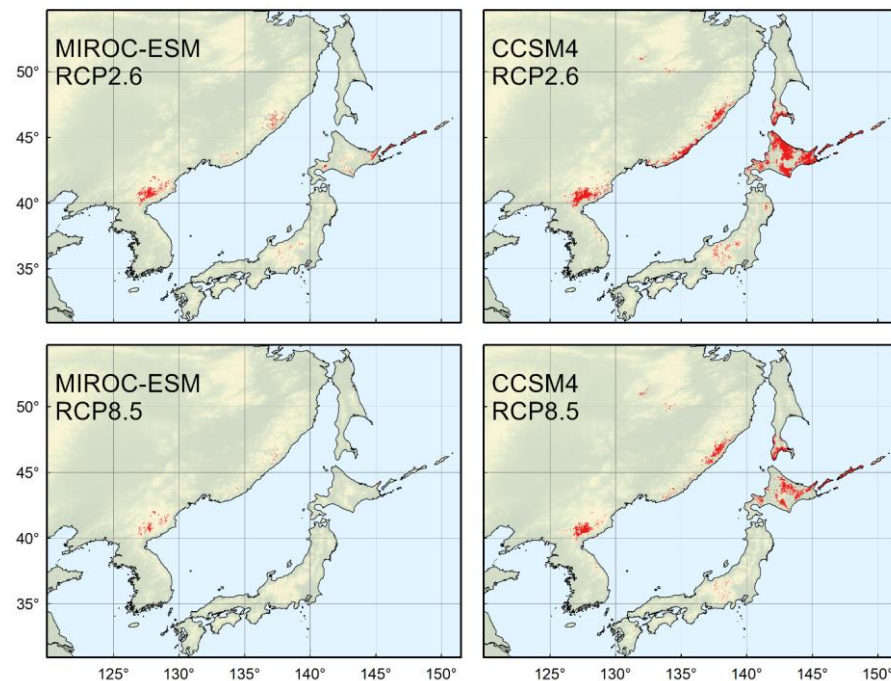


Figure 3. Overlay of *Picea jezoensis* (Siebold & Zucc.) Carrière potential distribution models of the four-time frames LGM-MHO-Current-Future follow the projected state of the MIROC-ESM and CCSM4 models and the RCP2.6 and RCP8.5 scenarios for the year 2070.

4. Discussion

4.1. Model of Current Distribution

In the continental part, *P. jezoensis* has an almost continuous range along the Pacific coast of Eurasia from 40 to 50° N. The ranges most distant from the seacoasts correspond to the Lesser Khingan Ranges and the Tukuringra Range. The climatic model predicted suitable areas for this species as relict isolated populations in the mountainous region of the Korean Peninsula, for the northern part of which there are only literature indications on the presence of *P. jezoensis* [54], but the presence points were absent in these locations according to our modeling protocols. Non-zero presence probabilities of *P. jezoensis* were obtained for several areas in South Korea, such as Mount Seorak (38.12° N, 128.46° E) and Mount Odae (37.80° N, 128.53° E), for which we had no presence points, but the *P. jezoensis* distribution is known from literature data [54]. On the other hand, the sensitivity of our model was not sufficient to predict the southernmost point of occurrence of *P. jezoensis* on Mount Jiri (35.33° N, 127.73° E).

Although we excluded the presence points of *P. jezoensis* subsp. *hondoensis* in central Honshu from the analysis, the mountainous areas where this taxon is commonly found were marked with a non-zero probability of presence. This region supports conditions for the existence of many other rare conifer taxa isolated from the main range besides *P. jezoensis*, for example, *Pinus koraiensis* Siebold & Zucc. [47].

4.2. Reconstructed Distribution in the LGM

The LGM climate in the region was characterized by lower temperatures and an arid environment [55]. Fundamentally different climatic conditions and different land contours during the sea level regression were reflected in a different distribution of biomes and their constituent species [56]. The MIROC-ESM and CCSM4 climate models provide generally similar climatic ranges of *P. jezoensis* during the LGM, with the main part of the species range located much further south than today, at 41–42° N. In addition to reflecting similar trends in bioclimatic extent, the two models are very different from each other: the MIROC-ESM predicted area is significantly smaller than that of the CCSM4. The climatically suitable area for the species according to the MIROC-ESM is somewhat smaller

and the CCSM4 is somewhat larger than the area of the modern climatic range. It should be considered that the total land area during the LGM was higher due to marine regression. In particular, the CCSM4 model predicts the area between modern Hokkaido and Sakhalin (the Soya Landbridge) as a climatically suitable area. The seabed in the form of coastal plains represented additional habitats [57].

According to the CCSM4 model, areas with suitable bioclimatic conditions for *P. jezoensis* up to 50° N were preserved along the coast of the Sea of Japan, the eastern slopes of the Sikhote-Alin Mountains, and the western coast of Sakhalin Island. In the MIROC-ESM model, the northern limits of the climatically acceptable area for the species are located much more south. Although vegetation reconstructions [56] carried out for the area north of 45° N imply the presence of sparse larch forests (tundra-like vegetation) and the landscape complex supporting the mammoth tundra–steppe vegetation [58,59], *P. jezoensis* is recorded in the palynological spectra of Sakhalin and Northeastern Hokkaido during the LGM [60,61]. At the same time, *Picea* (probably *P. jezoensis*) pollen is recorded in the Lake Khanka area (45° N 132° E) [62]. The continental regions of Northeastern China had an arid climate and, judging by pollen surveys, supported forest-steppe and shrub-steppe vegetation. Herbs expanded rapidly, dominated mainly by *Poaceae*. During the LGM, the forest in the northern part of Northeast China was relatively open and dominated by larches. Forests composed of birch, pine, and alder have developed in the Changbai Mountains [63]. Vegetation structure in areas with less arid climates closer to seacoasts was clearly more complex than in homogeneous larch forests, and areas of light coniferous taiga were interspersed with refugia of dark coniferous taiga [64], and the overall vegetation heterogeneity was supported by ample populations of megafauna [65].

The range of *P. jezoensis* was located much farther south in the climatic conditions of the LGM than at present (Figure 2). On the contrary, the current isolated area of *P. jezoensis* on the mainland in the central part of Kamchatka corresponds with the minimal influence of the sea within the whole peninsula, and in this zone, the so-called “coniferous forest island” is formed. Populations of *P. jezoensis* in Kamchatka are thought to be relict and have been preserved in this area since past warm epochs when the distribution area of *P. jezoensis* included the entire coast of the northern Okhotsk Sea. The time of isolation of the Kamchatka population of *P. jezoensis* is estimated to be more than 400 thousand years [32]. However, both models do not predict the preservation of climatic refugia of *P. jezoensis* in central Kamchatka, even though there is no doubt about the preservation of the species in this area since the interglacial period. According to [34], the Kamchatka Peninsula population of *P. jezoensis* was part of the mainland Asian range and separated during the mid-Pleistocene. We explain this by the insufficient accuracy of model reproduction for remote and sparsely populated areas of Northeast Asia.

The genetic structure of *P. jezoensis* on the mainland is closer to the population in the northern part of Sakhalin Island [35]. The southern part of the island is closer to Hokkaido Island, which was settled from the mainland by land bridges in the mid-Pleistocene. Analysis of microsatellite loci indicates that *P. jezoensis* populations in southern Sakhalin and Hokkaido have passed through a series of bottlenecks [35]. In the context of our modeling data, this clearly signals the existence of isolated refugia in Sakhalin and Hokkaido during the LGM period, as confirmed by palynological studies [60,61,66].

4.3. Reconstructed Distribution in the MHO

The MHO in the region was characterized by a higher temperature compared to the present, which was reflected in the expansion of mixed stands of the main plant species, including more thermophilic taxa, as evidenced by palynospectrum imprints [67,68]. Changes in climatic conditions in the region from the LGM to the MHO were accompanied by the transformation of natural complexes and changes in the boundaries of the main vegetation types. Warming and increased precipitation were accompanied by the northward expansion of the forest-forming species of the dark coniferous forests from more southern latitudes and isolated refugia. Simultaneously with the poleward expansion, populations

disappeared in the southern part of the range, where boreal and mixed forest ecosystems were replaced by more thermophilic vegetation [66,68,69].

The MIROC-ESM and CCSM4 models for the MHO climates predict smaller areas of *P. jezoensis* ranges than those under modern climates (Table 3). Both models show that in the MHO, the zone of a continuous distribution of *P. jezoensis* in mainland Northeast Asia was restricted to the southern Sikhote-Alin Mountains in the south, and the mountain ranges of North Korea and Northeast China (the Changbai Mountains) represented refugia separated from the main range. Palynological data from the southern Sikhote-Alin Mountains show that *P. jezoensis* did not disappear from plant communities during the LGM, but the proportion of pollen from this species was significantly lower than at present and was higher in broadleaved species [70,71]. In the island part of the region, the MHO was a period of a significant decrease in *P. jezoensis* pollen and an increase in the proportion of *Quercus mongolica* Fisch. ex Ledeb. s.l. pollen [61,66]. In the MHO time, relict populations of *P. jezoensis* subsp. *hondoensis* on Honshu and isolated populations of *P. jezoensis* in the mountains of the southern part of the Korean Peninsula have formed. At the same time, warmer climatic conditions in Kamchatka facilitated the spread of *P. jezoensis* from refugia preserved in the LGM [34,35].

4.4. Predicted Distribution in the Year 2070

RCP models ensure an increase in the temperature and precipitation balance depending on the concentration of greenhouse gases in the atmosphere. According to the optimistic scenario RCP2.6, the temperature increase by 2100 will be 2 °C, and according to the scenario RCP8.5 by 5 °C [28,29].

All scenarios and climate models for the year 2070 envisage more dramatic changes in the range of *P. jezoensis* than those that have occurred from the MHO to the present. In the RCP2.6 scenario, both the MIROC-ESM and CCSM4 project growth in areas of optimal climatic conditions. Areas in much of Kamchatka and along the coast of the Sea of Okhotsk will be suitable for the species. At the same time, a continuous area of climatically acceptable habitats in the southern part of the species range on the continent will disappear. A further reduction of potentially suitable areas will also occur in the extreme south of the species range, in the mountains of the southern Korean Peninsula [72,73]. Effects of climate change on coniferous tree species in the region have been observed [74–78]. Dendrochronological methods revealed a decline in the annual growth of *P. jezoensis* in China and Korea since 1980 in the lower elevations of the Changbai Mountains [79]. At the same time, an increase in the width of annual tree rings was observed in the higher elevations, as well as an extension of the length of the growing season.

Warming under the RCP8.5 scenario would result in an even more significant change in the contours of potentially suitable habitat for *P. jezoensis*, but while the projected area of the CCSM4 model would be higher than the current one, the MIROC-ESM model would reduce the final area of climatically suitable habitat.

Nevertheless, even the realization of the most pessimistic climate change scenarios will not cause the extinction of mainland populations in the Pektusan region (the southern face of the Changbai Mountains), which has an uninterrupted history since the LGM, and will not cause the complete disappearance of refugia in central Japan, although it will greatly reduce them.

The overlay of climatically acceptable areas for *P. jezoensis* from the LGM to the year 2070 shows that such areas are extremely small. Even the pessimistic RCP8.5 scenarios do not foresee the complete disappearance of *P. jezoensis* habitats from the Changbai Mountains, where populations of this species have existed continuously since the LGM. In the CCSM4 model, such areas of long-existing *P. jezoensis* include, in addition to the Changbai Mountains, central and southern parts of the Sikhote-Alin Mountains, partially, Hokkaido, southern Sakhalin, and southern Kurils (Figure 3).

4.5. Implications for Conservation and Management

It should be noted that modeling methods provide a probabilistic assessment of potential niches in terms of climate. Species distributions are affected by competition, dispersal, niche size, and environmental conditions in space and time [80]. Natural shifts in vegetation distribution may take longer because they depend on, among other things, the availability of diaspores, competitive relationships between plants, and local factors of a particular habitat [81,82]. At the same time, predictive models must always consider not only the extent of suitable habitats but also the rate of species distribution expansion, which is usually much slower than global climate change. The use of modeling techniques provides insight into trends in the general state of populations, allows planning of the conservation risks of *P. jezoensis* within the current range, and builds a systematic concept for creating forest crops and establishing forest plantations outside the current distribution of the species, with respect to expected climate changes [13,83,84].

To preserve the genetic diversity of *P. jezoensis* and intraspecific taxa, it is advisable to think about establishing plantations in places where the climate will be acceptable in the long term and in the context of projected changes. Forestry must take climate trends into account when establishing new plantations of *P. jezoensis*. Establishing artificial forest stands of this species in the southern part of its range against the background of a changing climate appears to be a bad decision, while a deeper introduction of this species into forestry practices could be a very prudent decision for areas of Northeast Asia where *P. jezoensis* does not currently grow in natural ecosystems.

The departure of *P. jezoensis* populations from the optimal climate zone will not cause their one-step extinction but will determine a trend towards gradual extinction by increased tree elimination due to bacterial diseases, fungal diseases, limitation of natural regeneration processes, drought, and fires accompanying drought. Within the study region, the previously unknown occurrence of bark beetle outbreaks took place in the Sakhalin and Kuril Islands as a result of massive windthrows in spruce and fir forests [85–87].

Due to the genetic diversity found in the populations of the species [32–35] and in order to preserve it, it is necessary to create stands of *P. jezoensis* from those places where the extinction of species is assumed. Such work cannot be carried out within one country and will require the consolidation of the efforts of all the states of Northeast Asia into a common project. The genetic structure of local populations of *P. jezoensis* in the mainland part of the species range has not been sufficiently studied, in contrast to detailed studies on the Japanese islands. First, it is of interest to collect materials from the boundaries of the modern distribution of the species on the Sikhote-Alin Mountains, the Lesser Khingan Mountains, the Tukuringra Range, and the southern Kurils.

5. Conclusions

SDMs of *P. jezoensis* built in this study are based on five bioclimatic factors and considered the distribution of climate continentality, heat balance throughout the year, and precipitation in warm and cold periods. The area of current suitable climatic conditions for *P. jezoensis* is estimated at more than 500,000 km². The MIROC-ESM and CCSM4 climate models for retrospective and predictive modeling provide slightly different estimates of potential range but describe similar trends in species range shifts.

We identify areas in the Changbai Mountains (China, North Korea) and the Sikhote-Alin Mountains (Russia) as long-term climatically stable *P. jezoensis* refugia from the LGM to projective climate conditions of the year 2070 under the scenario RCP8.5. These areas could be prioritized for the in situ conservation of species populations. In addition to its ecosystem role, *P. jezoensis* is also an economically important species, so the obtained results should also be applied in forestry planning. Potentially favorable climatic areas in the northern parts of Northeast Asia according to the obtained models should be considered and used as places for establishing artificial forest stands of *P. jezoensis* in the future. A reforestation process using *P. jezoensis* and commercial planting does not have long-term perspectives in more southern areas.

Supplementary Materials: The following supporting information can be downloaded at <https://www.mdpi.com/article/10.3390/f14020219/s1>, Figure S1: Distribution maps of *Picea jezoensis* (a) by Manko (1987); (b), Nakamura and Krestov (2005); (c) Aizawa et al., 2009.

Author Contributions: Conceptualization, K.K. and T.P.; methodology, D.K., software, D.K.; validation, K.K., T.P. and D.K.; formal analysis, T.P.; data curation, D.K.; writing—original draft preparation, T.P.; writing—review and editing, K.K., D.K., P.K. and J.D.; visualization, K.K., T.P. and D.K.; supervision, P.K. and J.D.; funding acquisition, K.K., P.K. and J.D. All authors have read and agreed to the published version of the manuscript.

Funding: This work was funded by the Ministry of Education, Youth and Sport of the Czech Republic (MŠMT), the project Mobility 2020 (CZ.02.2.69/0.0/0.0/18_053/0017850), K.K.; the Czech Science Foundation (20-05840Y), K.K.; (21-26883S), J.D.; long-term research development project of the Czech Academy of Sciences (RVO 67985939), K.K. and J.D.; the scientific research project of the Botanical Garden-Institute FEB RAS (FWFR-2022-0008) No. 122040800089-2, P.K.

Data Availability Statement: Data The data presented in this study are available in the article.

Conflicts of Interest: The authors declare no conflict of interest.

References

- Chen, I.-C.; Hill, J.K.; Ohlemüller, R.; Roy, D.B.; Thomas, C.D. Rapid Range Shifts of Species Associated with High Levels of Climate Warming. *Science* **2011**, *333*, 1024–1026. [[CrossRef](#)]
- Becknell, J.M.; Desai, A.R.; Dietze, M.C.; Schultz, C.A.; Starr, G.; Duffy, P.A.; Franklin, J.F.; Pourmokhtarian, A.; Hall, J.; Stoy, P.C.; et al. Assessing Interactions Among Changing Climate, Management, and Disturbance in Forests: A Macrosystems Approach. *Bioscience* **2015**, *65*, 263–274. [[CrossRef](#)]
- Seidl, R.; Thom, D.; Kautz, M.; Martin-Benito, D.; Peltoniemi, M.; Vacchiano, G.; Wild, J.; Ascoli, D.; Petr, M.; Honkaniemi, J.; et al. Forest disturbances under climate change. *Nat. Clim. Chang.* **2017**, *7*, 395–402. [[CrossRef](#)] [[PubMed](#)]
- Guisan, A.; Zimmermann, N.E. Predictive habitat distribution models in ecology. *Ecol. Model.* **2000**, *135*, 147–186. [[CrossRef](#)]
- Elith, J.H.; Graham, C.P.H.; Anderson, R.P.; Dudík, M.; Ferrier, S.; Guisan, A.; Hijmans, R.J.; Huettmann, F.; Leathwick, J.R.; Lehmann, A.; et al. Novel methods improve prediction of species' distributions from occurrence data. *Ecography* **2006**, *29*, 129–151. [[CrossRef](#)]
- Elith, J.; Leathwick, J.R. Species Distribution Models: Ecological Explanation and Prediction Across Space and Time. *Annu. Rev. Ecol. Syst.* **2009**, *40*, 677–697. [[CrossRef](#)]
- Kearney, M.; Porter, W. Mechanistic niche modelling: Combining physiological and spatial data to predict species' ranges. *Ecol. Lett.* **2009**, *12*, 334–350. [[CrossRef](#)]
- Pearson, R.G.; Dawson, T.P. Predicting the impacts of climate change on the distribution of species: Are bioclimate envelope models useful? *Glob. Ecol. Biogeogr.* **2003**, *12*, 361–371. [[CrossRef](#)]
- Hijmans, R.J.; Graham, C.H. The ability of climate envelope models to predict the effect of climate change on species distributions. *Glob. Chang. Biol.* **2006**, *12*, 2272–2281. [[CrossRef](#)]
- Booth, T.H. Species distribution modelling tools and databases to assist managing forests under climate change. *For. Ecol. Manag.* **2018**, *430*, 196–203. [[CrossRef](#)]
- Santini, L.; Benítez-López, A.; Maiorano, L.; Čengić, M.; Huijbregts, M.A.J. Assessing the reliability of species distribution projections in climate change research. *Divers. Distrib.* **2021**, *27*, 1035–1050. [[CrossRef](#)]
- Tang, C.Q.; Matsui, T.; Ohashi, H.; Dong, Y.-F.; Momohara, A.; Herrando-Moraira, S.; Qian, S.; Yang, Y.; Ohsawa, M.; Luu, H.T.; et al. Identifying long-term stable refugia for relict plant species in East Asia. *Nat. Commun.* **2018**, *9*, 4488. [[CrossRef](#)] [[PubMed](#)]
- Janowiak, M.K.; Swanston, C.; Nagel, L.M.; Brandt, L.A.; Butler, P.R.; Handler, S.D.; Shannon, P.D.; Iverson, L.R.; Matthews, S.; Prasad, A.; et al. A Practical Approach for Translating Climate Change Adaptation Principles into Forest Management Actions. *J. For.* **2014**, *112*, 424–433. [[CrossRef](#)]
- Schelhaas, M.-J.; Nabuurs, G.-J.; Hengeveld, G.; Reyer, C.; Hanewinkel, M.; Zimmermann, N.E.; Cullmann, D. Alternative forest management strategies to account for climate change-induced productivity and species suitability changes in Europe. *Reg. Environ. Chang.* **2015**, *15*, 1581–1594. [[CrossRef](#)]
- Krestov, P.V. Forest Vegetation of Easternmost Russia (Russian Far East). In *Forest Vegetation of Northeast Asia. Geobotany*; Kolbek, J., Šrútek, M., Box, E.O., Eds.; Springer: Dordrecht, The Netherlands, 2003; Volume 28, pp. 93–180.
- Manko, Y.I. *El' Ajanskaya (Picea Ajanensis)*; Nauka: Leningrad, Russia, 1987. (In Russian)
- Shao, C.-C.; Shen, T.-T.; Jin, W.-T.; Mao, H.-J.; Ran, J.-H.; Wang, X.-Q. Phylotranscriptomics resolves interspecific relationships and indicates multiple historical out-of-North America dispersals through the Bering Land Bridge for the genus *Picea* (Pinaceae). *Mol. Phylogenet. Evol.* **2019**, *141*, 106610. [[CrossRef](#)] [[PubMed](#)]

18. Nakamura, Y.; Krestov, P.V. Coniferous forests of the temperate zone of Asia. *Coniferous forests. Ser. Ecosyst. World* **2005**, *6*, 163–220.
19. Allen, C.D.; Macalady, A.K.; Chenchouni, H.; Bachelet, D.; McDowell, N.; Vennetier, M.; Kitzberger, T.; Rigling, A.; Breshears, D.D.; Hogg, E.H.; et al. A global overview of drought and heat-induced tree mortality reveals emerging climate change risks for forests. *For. Ecol. Manag.* **2010**, *259*, 660–684. [[CrossRef](#)]
20. Gauthier, S.; Bernier, P.; Kuuluvainen, T.; Shvidenko, A.Z.; Schepaschenko, D.G. Boreal forest health and global change. *Science* **2015**, *349*, 819–822. [[CrossRef](#)]
21. Kuuluvainen, T.; Gauthier, S. Young and old forest in the boreal: Critical stages of ecosystem dynamics and management under global change. *For. Ecosyst.* **2018**, *5*, 26. [[CrossRef](#)]
22. Svenning, J.-C.; Eiserhardt, W.L.; Normand, S.; Ordonez, A.; Sandel, B. The Influence of Paleoclimate on Present-Day Patterns in Biodiversity and Ecosystems. *Annu. Rev. Ecol. Evol. Syst.* **2015**, *46*, 551–572. [[CrossRef](#)]
23. Hijmans, R.J.; Cameron, S.E.; Parra, J.L.; Jones, P.G.; Jarvis, A. Very high resolution interpolated climate surfaces for global land areas. *Int. J. Climatol.* **2005**, *25*, 1965–1978. [[CrossRef](#)]
24. WorldClim. 1.4 Downscaled Paleo Climate. Available online: <https://www.worldclim.org/data/v1.4/paleo1.4.html> (accessed on 17 January 2023).
25. Watanabe, S.; Hajima, T.; Sudo, K.; Nagashima, T.; Takemura, T.; Okajima, H.; Nozawa, T.; Kawase, H.; Abe, M.; Yokohata, T.; et al. MIROC-ESM 2010: Model description and basic results of CMIP5-20c3m experiments. *Geosci. Model Dev.* **2011**, *4*, 845–872. [[CrossRef](#)]
26. Kawamiya, M.; Hajima, T.; Tachiiri, K.; Watanabe, S.; Yokohata, T. Two decades of Earth system modeling with an emphasis on Model for Interdisciplinary Research on Climate (MIROC). *Prog. Earth Planet. Sci.* **2020**, *7*, 64. [[CrossRef](#)]
27. Gent, P.R.; Danabasoglu, G.; Donner, L.J.; Holland, M.M.; Hunke, E.C.; Jayne, S.R.; Lawrence, D.M.; Neale, R.B.; Rasch, P.J.; Vertenstein, M.; et al. The Community Climate System Model Version 4. *J. Clim.* **2011**, *24*, 4973–4991. [[CrossRef](#)]
28. Van Vuuren, D.P.; Stehfest, E.; den Elzen, M.G.J.; Kram, T.; Van Vliet, J.; Deetman, S.; Isaac, M.; Goldewijk, K.K.; Hof, A.; Beltran, A.M.; et al. RCP2.6: Exploring the possibility to keep global mean temperature increase below 2 °C. *Clim. Chang.* **2011**, *109*, 95–116. [[CrossRef](#)]
29. Riahi, K.; Rao, S.; Krey, V.; Cho, C.; Chirkov, V.; Fischer, G.; Kindermann, G.E.; Nakicenovic, N.; Rafaj, P. RCP 8.5—A scenario of comparatively high greenhouse gas emissions. *Clim. Chang.* **2011**, *109*, 33–57. [[CrossRef](#)]
30. Rokach, L.; Maimon, M.O. Classification Trees. In *Data Mining and Knowledge Discovery Handbook*; Maimon, O., Rokach, L., Eds.; Springer: Boston, MA, USA, 2009; pp. 149–174.
31. Krestov, P.V.; Nakamura, Y. Phytosociological study of the *Picea jezoensis* forests of the far east. *Folia Geobot.* **2002**, *37*, 441–473. [[CrossRef](#)]
32. Potenko, V.V.; Knysh, Y.D. Genetic variation of Yeddo spruce populations in Russia. *For. Genet.* **2003**, *10*, 55–64.
33. Potenko, V.V. Allozyme Variation and Phylogenetic Relationships in *Picea jezoensis* (Pinaceae) Populations of the Russian Far East. *Biochem. Genet.* **2007**, *45*, 291–304. [[CrossRef](#)]
34. Aizawa, M.; Yoshimaru, H.; Saito, H.; Katsuki, T.; Kawahara, T.; Kitamura, K.; Shi, F.; Kaji, M. Phylogeography of a northeast Asian spruce, *Picea jezoensis*, inferred from genetic variation observed in organelle DNA markers. *Mol. Ecol.* **2007**, *16*, 3393–3405. [[CrossRef](#)]
35. Aizawa, M.; Yoshimaru, H.; Saito, H.; Katsuki, T.; Kawahara, T.; Kitamura, K.; Shi, F.; Sabirov, R.; Kaji, M. Range-wide genetic structure in a north-east Asian spruce (*Picea jezoensis*) determined using nuclear microsatellite markers. *J. Biogeogr.* **2009**, *36*, 996–1007. [[CrossRef](#)]
36. GBIF. Global Biodiversity Information Facility. Available online: <https://www.gbif.org/> (accessed on 9 October 2022).
37. GeoPy's Documentation. Available online: <https://geopy.readthedocs.io/en/stable/> (accessed on 9 October 2022).
38. Average Nearest Neighbor, ArcMap 10.8. Available online: <https://desktop.arcgis.com/en/arcmap/latest/tools/spatial-statistics-toolbox/average-nearest-neighbor.htm> (accessed on 9 October 2022).
39. Nakamura, Y.; Krestov, P.V.; Omelko, A.M. Bioclimate and zonal vegetation in Northeast Asia: First approximation to an integrated study. *Phytocoenologia* **2007**, *37*, 443–470. [[CrossRef](#)]
40. Noce, S.; Caporaso, L.; Santini, M. A new global dataset of bioclimatic indicators. *Sci. Data* **2020**, *7*, 398. [[CrossRef](#)] [[PubMed](#)]
41. NumPy. The Fundamental Package for Scientific Computing with Python. Available online: <https://numpy.org/> (accessed on 9 October 2022).
42. Imdadullah, M.; Aslam, M.; Altaf, S. mctest: An R Package for Detection of Collinearity among Regressors. *R J.* **2016**, *8*, 495–505. [[CrossRef](#)]
43. GDAL Documentation. Available online: <https://gdal.org/> (accessed on 9 October 2022).
44. Pedregosa, F.; Varoquaux, G.; Gramfort, A.; Michel, V.; Thirion, B.; Grisel, O.; Blondel, M.; Prettenhofer, P.; Weiss, R.; Dubourg, V.; et al. Scikit-learn: Machine learning in Python. *J. Mach. Learn. Res.* **2011**, *12*, 2825–2830. [[CrossRef](#)]
45. Čengić, M.; Rost, J.; Remenska, D.; Janse, J.H.; Huijbregts, M.A.J.; Schipper, A.M. On the importance of predictor choice, modelling technique, and number of pseudo-absences for bioclimatic envelope model performance. *Ecol. Evol.* **2020**, *10*, 12307–12317. [[CrossRef](#)]
46. Zhao, Z.; Xiao, N.; Shen, M.; Li, J. Comparison between optimized MaxEnt and random forest modeling in predicting potential distribution: A case study with *Quasipaa boulengeri* in China. *Sci. Total Environ.* **2022**, *842*, 156867. [[CrossRef](#)] [[PubMed](#)]

47. Petrenko, T.Y.; Korznikov, K.A.; Kislov, D.E.; Belyaeva, N.G.; Krestov, P.V. Modeling of cold-temperate tree *Pinus koraiensis* (Pinaceae) distribution in the Asia-Pacific region: Climate change impact. *For. Ecosyst.* **2022**, *9*, 100015. [[CrossRef](#)]
48. Boyce, M.S.; Vernier, P.R.; E. Nielsen, S.; Schmiegelow, F.K. Evaluating resource selection functions. *Ecol. Model.* **2002**, *157*, 281–300. [[CrossRef](#)]
49. Lobo, J.M.; Jiménez-Valverde, A.; Real, R. AUC: A misleading measure of the performance of predictive distribution models. *Glob. Ecol. Biogeogr.* **2007**, *17*, 145–151. [[CrossRef](#)]
50. Breiman, L. Random forests. *Mach. Learn.* **2001**, *45*, 5–32. [[CrossRef](#)]
51. Liu, C.; White, M.; Newell, G. Selecting thresholds for the prediction of species occurrence with presence-only data. *J. Biogeogr.* **2013**, *40*, 778–789. [[CrossRef](#)]
52. Konowalik, K.; Nosol, A. Evaluation metrics and validation of presence-only species distribution models based on distributional maps with varying coverage. *Sci. Rep.* **2021**, *11*, 1482. [[CrossRef](#)]
53. USGS EROS Archive—Digital Elevation—Shuttle Radar Topography Mission (SRTM) 1 Arc-Second Global. Available online: <https://www.usgs.gov/centers/eros/science/usgs-eros-archive-digital-elevation-shuttle-radar-topography-mission-srtm-1> (accessed on 9 October 2022).
54. Černý, T.; Kopecký, M.; Petřík, P.; Song, J.-S.; Šrůtek, M.; Valachovič, M.; Altman, J.; Doležal, J. Classification of Korean forests: Patterns along geographic and environmental gradients. *Appl. Veg. Sci.* **2014**, *18*, 5–22. [[CrossRef](#)]
55. Herzsuh, U.; Birks, H.J.B.; Laepple, T.; Andreev, A.; Melles, M.; Brigham-Grette, J. Glacial legacies on interglacial vegetation at the Pliocene-Pleistocene transition in NE Asia. *Nat. Commun.* **2016**, *7*, 11967. [[CrossRef](#)]
56. Tsukada, M. *Vegetation in prehistoric Japan: The last 20,000 years*, In *Windows on the Japanese Past: Studies in Archeology and Prehistory*; Center for Japanese Studies, University of Michigan: Ann Arbor, MI, USA, 1986; pp. 11–56.
57. Sakaguchi, S.; Sakurai, S.; Yamasaki, M.; Isagi, Y. How did the exposed seafloor function in postglacial northward range expansion of *Kalopanax septemlobus*? Evidence from ecological niche modelling. *Ecol. Res.* **2010**, *25*, 1183–1195. [[CrossRef](#)]
58. Vereshchagin, N.K.; Baryshnikov, G.F. The ecological structure of the “Mammoth Fauna” in Eurasia. *Ann. Zool. Fenn.* **1991**, *28*, 253–259. Available online: <https://www.jstor.org/stable/23735450> (accessed on 9 October 2022).
59. Markova, A.K.; Smirnov, N.G.; Kozharinov, A.V.; Kazantseva, N.E.; Simakova, A.N.; Kitaev, L.M. Late Pleistocene distribution and diversity of mammals in Northern Eurasia (PALEOFAUNA database). *Paleontol. Evol.* **1995**, *28–29*, 5–66.
60. Igarashi, Y.; Zharov, A.E. Climate and vegetation change during the late Pleistocene and early Holocene in Sakhalin and Hokkaido, northeast Asia. *Quat. Int.* **2011**, *237*, 24–31. [[CrossRef](#)]
61. Igarashi, Y. Vegetation and climate during the LGM and the last deglaciation on Hokkaido and Sakhalin Islands in the northwest Pacific. *Quat. Int.* **2016**, *425*, 28–37. [[CrossRef](#)]
62. Belyanin, P.S.; Belyanina, N.I. On the Prikhanka depression vegetation cover evolution and its mountain framing in the Late Neopleistocene-Holocene (from palynological data). *Russ. J. Pac. Geol.* **2012**, *31*, 96–108. (In Russian)
63. Li, X.; Zhao, C.; Zhou, X. Vegetation pattern of Northeast China during the special periods since the Last Glacial Maximum. *Sci. China Earth Sci.* **2019**, *62*, 1224–1240. [[CrossRef](#)]
64. Herzsuh, U. Legacy of the Last Glacial on the present-day distribution of deciduous versus evergreen boreal forests. *Glob. Ecol. Biogeogr.* **2019**, *29*, 198–206. [[CrossRef](#)]
65. Zimov, S.; Zimov, N.; Tikhonov, A.; Chapin, F. Mammoth steppe: A high-productivity phenomenon. *Quat. Sci. Rev.* **2012**, *57*, 26–45. [[CrossRef](#)]
66. Ooi, N. Vegetation history of Japan since the last glacial based on palynological data. *Jpn. J. Hist. Bot.* **2016**, *25*, 1–101. [[CrossRef](#)]
67. Cao, X.; Herzsuh, U.; Ni, J.; Zhao, Y.; Böhmer, T. Spatial and temporal distributions of major tree taxa in eastern continental Asia during the last 22,000 years. *Holocene* **2014**, *25*, 79–91. [[CrossRef](#)]
68. Binney, H.; Edwards, M.; Macias-Fauria, M.; Lozhkin, A.; Anderson, P.; Kaplan, J.O.; Andreev, A.; Bezrukova, E.; Blyakharchuk, T.; Jankovska, V.; et al. Vegetation of Eurasia from the last glacial maximum to present: Key biogeographic patterns. *Quat. Sci. Rev.* **2017**, *157*, 80–97. [[CrossRef](#)]
69. Zhao, C.; Li, X.; Zhou, X.; Zhao, K.; Yang, Q. Holocene vegetation succession and responses to climate change in the northern sector of Northeast China. *Sci. China Earth Sci.* **2016**, *59*, 1390–1400. [[CrossRef](#)]
70. Razjigaeva, N.; Ganzey, L.; Grebennikova, T.; Mokhova, L.; Kudryavtseva, E.; Arslanov, K.; Maksimov, F.; Starikova, A. Landscape and environmental changes along the Eastern Primorye coast during the middle to late Holocene and human effects. *J. Asian Earth Sci.* **2018**, *158*, 160–172. [[CrossRef](#)]
71. Razjigaeva, N.; Ganzey, L.; Lyashevskaya, M.; Makarova, T.; Kudryavtseva, E.; Grebennikova, T.; Panichev, A.; Arslanov, K.; Maksimov, F.; Petrov, A.Y.; et al. Climatic and human impacts on landscape development of the Murav’ev Amursky Peninsula (Russian South Far East) in the Middle/Late Holocene and historical time. *Quat. Int.* **2019**, *516*, 127–140. [[CrossRef](#)]
72. Jang, W.; Park, P.S. Stand Structure and Maintenance of *Picea jezoensis* in a Northern Temperate Forest, South Korea. *J. Plant Biol.* **2010**, *53*, 180–189. [[CrossRef](#)]
73. Jang, W.; Keyes, C.R.; Running, S.W.; Lim, J.-H.; Park, P.S. Climate–growth relationships of relict *Picea jezoensis* at Mt. Gyeong, South Korea. *For. Sci. Technol.* **2014**, *11*, 19–26. [[CrossRef](#)]
74. Yu, D.; Wang, Q.; Wang, Y.; Zhou, W.; Ding, H.; Fang, X.; Jiang, S.; Dai, L. Climatic effects on radial growth of major tree species on Changbai Mountain. *Ann. For. Sci.* **2011**, *68*, 921–933. [[CrossRef](#)]

75. Wang, H.; Shao, X.-M.; Jiang, Y.; Fang, X.-Q.; Wu, S.-H. The impacts of climate change on the radial growth of *Pinus koraiensis* along elevations of Changbai Mountain in northeastern China. *For. Ecol. Manag.* **2013**, *289*, 333–340. [[CrossRef](#)]
76. Gai, X.; Wang, S.; Zhou, L.; Wu, J.; Zhou, W.; Bi, J.; Cao, L.; Dai, L.; Yu, D. Spatiotemporal evidence of tree-growth resilience to climate variations for Yezo spruce (*Picea jezoensis* var. *komarovii*) on Changbai Mountain, Northeast China. *J. For. Res.* **2018**, *31*, 927–936. [[CrossRef](#)]
77. Hiura, T.; Go, S.; Iijima, H. Long-term forest dynamics in response to climate change in northern mixed forests in Japan: A 38-year individual-based approach. *For. Ecol. Manag.* **2019**, *449*, 117469. [[CrossRef](#)]
78. Kim, E.S.; Lee, J.S.; Park, G.E.; Lim, J.-H. Change of subalpine coniferous forest area over the last 20 years. *J. Korean Soc. For. Sci.* **2019**, *108*, 10–20. [[CrossRef](#)]
79. Zhu, L.; Cooper, D.J.; Yang, J.; Zhang, X.; Wang, X. Rapid warming induces the contrasting growth of Yezo spruce (*Picea jezoensis* var. *microsperma*) at two elevation gradient sites of northeast China. *Dendrochronologia* **2018**, *50*, 52–63. [[CrossRef](#)]
80. Pulliam, H. On the relationship between niche and distribution. *Ecol. Lett.* **2000**, *3*, 349–361. [[CrossRef](#)]
81. Michalet, R.; Maalouf, J.-P.; Choler, P.; Clément, B.; Rosebery, D.; Royer, J.-M.; Schöb, C.; Lortie, C. Competition, facilitation and environmental severity shape the relationship between local and regional species richness in plant communities. *Ecography* **2014**, *38*, 335–345. [[CrossRef](#)]
82. Antúnez, P. Main environmental variables influencing the abundance of plant species under risk category. *J. For. Res.* **2021**, *33*, 1209–1217. [[CrossRef](#)]
83. Kolström, M.; Lindner, M.; Vilén, T.; Maroschek, M.; Seidl, R.; Lexer, M.J.; Netherer, S.; Kremer, A.; Delzon, S.; Barbati, A.; et al. Reviewing the Science and Implementation of Climate Change Adaptation Measures in European Forestry. *Forests* **2011**, *2*, 961–982. [[CrossRef](#)]
84. Jandl, R.; Spathelf, P.; Bolte, A.; Prescott, C.E. Forest adaptation to climate change—Is non-management an option? *Ann. For. Sci.* **2019**, *76*, 48. [[CrossRef](#)]
85. Vozmishcheva, A.S.; Bondarchuk, S.N.; Gromyko, M.N.; Kislov, D.E.; Pimenova, E.A.; Salo, M.A.; Korznikov, K.A. Strong Disturbance Impact of Tropical Cyclone Lionrock (2016) on Korean Pine-Broadleaved Forest in the Middle Sikhote-Alin Mountain Range, Russian Far East. *Forests* **2019**, *10*, 1017. [[CrossRef](#)]
86. Kislov, D.E.; Korznikov, K.A.; Altman, J.; Vozmishcheva, A.S.; Krestov, P.V. Extending deep learning approaches for forest disturbance segmentation on very high-resolution satellite images. *Remote Sens. Ecol. Conserv.* **2021**, *7*, 355–368. [[CrossRef](#)]
87. Korznikov, K.; Kislov, D.; Doležal, J.; Petrenko, T.; Altman, J. Tropical cyclones moving into boreal forests: Relationships between disturbance areas and environmental drivers. *Sci. Total Environ.* **2022**, *844*, 156931. [[CrossRef](#)]

Disclaimer/Publisher’s Note: The statements, opinions and data contained in all publications are solely those of the individual author(s) and contributor(s) and not of MDPI and/or the editor(s). MDPI and/or the editor(s) disclaim responsibility for any injury to people or property resulting from any ideas, methods, instructions or products referred to in the content.